Supplemental Material for Femtosecond valley polarization and topological resonances in transition metal dichalcogenides

S. Azar Oliaei Motlagh, Jhih-Sheng Wu, Vadym Apalkov, and Mark I. Stockman
Center for Nano-Optics (CeNO) and Department of Physics and Astronomy, Georgia State University, Atlanta, Georgia 30303, USA
(Dated: August 7, 2018)

I. TIGHT BINDING HAMILTONIAN

The three band third-nearest-neighbor (TNN) tight-binding (TB) model Hamiltonian, $H^{\rm TNN}$, of a transition metal dichalcogenide (TMDC) monolayer is constructed from three orbitals (d_{z^2}, d_{xy}, and $d_{x^2-y^2}$) of the metal atom, as introduced by Liu et al.[1], is

$$H^{\rm TNN}(\mathbf{k}) = \begin{bmatrix} V_0 & V_1 & V_2 \\ V_1^* & V_{11} & V_{12} \\ V_2^* & V_{12}^* & V_{22} \end{bmatrix} , \tag{1}$$

where

$$\begin{aligned}
V_0 &= \epsilon_1 + 2t_0(2\cos\alpha\cos\beta + \cos 2\alpha) + 2r_0(2\cos 3\alpha\cos\beta + \cos 2\beta) + 2u_0(2\cos 2\alpha\cos 2\beta + \cos 4\alpha) \ , \\
{\rm Re}[V_1] &= -2\sqrt{3}t_2\sin\alpha\sin\beta + 2(r_1+r_2)\sin 3\alpha\sin\beta - 2\sqrt{3}u_2\sin 2\alpha\sin 2\beta \ , \\
{\rm Im}[V_1] &= 2t_1\sin\alpha(2\cos\alpha + \cos\beta) + 2(r_1-r_2)\sin 3\alpha\cos\beta + 2u_1\sin 2\alpha(2\cos 2\alpha + \cos 2\beta) \ , \\
{\rm Re}[V_2] &= 2t_2(\cos 2\alpha - \cos\alpha\cos\beta) - \frac{2}{\sqrt{3}}(r_1+r_2)(\cos 3\alpha\cos\beta - \cos 2\beta) + 2u_2(\cos 4\alpha - \cos 2\alpha\cos 2\beta) \ , \\
{\rm Im}[V_2] &= 2\sqrt{3}t_1\cos\alpha\sin\beta + \frac{2}{\sqrt{3}}\sin\beta(r_1-r_2)(\cos 3\alpha + 2\cos\beta) + 2\sqrt{3}u_1\cos 2\alpha\sin 2\beta \ , \\
V_{11} &= \epsilon_2 + (t_{11}+3t_{22})\cos\alpha\cos\beta + 2t_{11}\cos 2\alpha + 4r_{11}\cos 3\alpha\cos\beta + 2(r_{11}+\sqrt{3}r_{12}\cos 2\beta) + \\
&\quad (u_{11}+3u_{22})\cos 2\alpha\cos 2\beta + 2u_{11}\cos 4\alpha \ , \\
{\rm Re}[V_{12}] &= \sqrt{3}(t_{22}-t_{11})\sin\alpha sin\beta + 4r_{12}\sin 3\alpha\sin\beta + \sqrt{3}(u_{22}-u_{11}\sin 2\alpha\sin 2\beta) \ , \\
{\rm Im}[V_{12}] &= 4t_{12}\sin\alpha(\cos\alpha - cos\beta) + 4u_{12}\sin 2\alpha(\cos 2\alpha - \cos 2\beta) \ , \\
V_{22} &= \epsilon_2 + (3t_{11}+t_{22})\cos\alpha\cos\beta + 2t_{22}\cos 2\alpha + 2r_{11}(2\cos 3\alpha\cos\beta + \cos 2\beta) + \\
&\quad \frac{2}{\sqrt{3}}r_{12}(4\cos 3\alpha\cos\beta - \cos 2\beta) + (3u_{11}+u_{22})\cos 2\alpha\cos 2\beta + 2u_{22}\cos 4\alpha \ ,
\end{aligned} \tag{2}$$

in which

$$(\alpha,\beta) = \left(\frac{1}{2}k_x a, \frac{\sqrt{3}}{2}k_y a\right) . \tag{3}$$

The values for parameters $a, \epsilon_1, \epsilon_2, t_0, t_1, t_2, t_{11}, t_{12}, t_{22}, r_0, r_1, r_2, r_{11}, r_{12}, u_0, u_1, u_2, u_{11}, u_{12}, u_{22}$ for MoS_2 and WS_2 can be found in the Table I.

II. SOC CONTRIBUTION TO THE HAMILTONIAN

The contribution of the spin orbit coupling (SOC), $H^{\rm SOC}$, to the total Hamiltonian written in the basis of $\{|d_{z^2},\uparrow\rangle, |d_{xy},\uparrow\rangle, |d_{x^2-y^2},\uparrow\rangle, |d_{z^2},\downarrow\rangle, |d_{xy},\downarrow\rangle, |d_{x^2-y^2},\downarrow\rangle\}$ is the following matrix[1,2] :

$$H^{\rm SOC} = \lambda \mathbf{L}.\mathbf{S} = \begin{bmatrix} \frac{\lambda}{2}L_z & 0 \\ 0 & -\frac{\lambda}{2}L_z \end{bmatrix} \tag{4}$$

	a	ϵ_1	ϵ_2	t_0	t_1	t_2	t_{11}
	t_{12}	t_{22}	r_0	r_1	r_2	r_{11}	r_{12}
	u_0	u_1	u_2	u_{11}	u_{12}	u_{22}	λ
MoS_2	3.190	0.683	1.707	-0.146	-0.114	0.506	0.085
	0.162	0.073	0.060	-0.236	0.067	0.016	0.087
	-0.038	0.046	0.001	0.266	-0.176	-0.150	0.073
WS_2	3.191	0.717	1.916	-0.152	-0.097	0.590	0.047
	0.178	0.016	0.069	-0.261	0.107	-0.003	0.109
	-0.054	0.045	0.002	0.325	-0.206	-0.163	0.211

TABLE I. Fitted parameters for three band TNN TB on the first-principles (FP) band structure in generalized-gradient approximation (GGA) case, lattice constant(a), and SOC paramrter (λ). All quantities are in unit eV except a which is in unit Å^1.

where λ is the SOC parameter, and L_z is the z-component of the orbital angular momentum[1],

$$L_z = \begin{bmatrix} 0 & 0 & 0 \\ 0 & 0 & 2i \\ 0 & -2i & 0 \end{bmatrix}. \tag{5}$$

Therefore, H^{SOC} is 2×2 block diagonal Hamiltonian where the nonzero upper block corresponds to spin up and the nonzero lower block corresponds to spin down[1].

III. MAIN EQUATIONS

The total Hamiltonian, $H_0(\mathbf{k})$, in the same basis is

$$H_0(\mathbf{k}) = H^{\text{TNN}}(\mathbf{k}) + H^{\text{SOC}} \tag{6}$$

where $H^{\text{TNN}}(\mathbf{k})$ is the 3×3 tight binding Hamiltonian without spin, $H^{\text{SOC}}(\mathbf{k})$ is the SOC contribution, and the total Hamiltonian, $H_0(\mathbf{k})$, is a block diagonal operator expressed as

$$H_0(\mathbf{k}) = \begin{bmatrix} H^{\text{TNN}}(\mathbf{k}) + \frac{\lambda}{2}L_z & 0 \\ 0 & H^{\text{TNN}}(\mathbf{k}) - \frac{\lambda}{2}L_z \end{bmatrix} = \begin{bmatrix} H^{\uparrow}_{3\times3}(\mathbf{k}) & 0 \\ 0 & H^{\downarrow}_{3\times3}(\mathbf{k}) \end{bmatrix}, \tag{7}$$

in which the nonzero upper block corresponds to the spin up and the nonzero lower block to the spin down. Band structures of MoS_2 and WS_2 for the two components of the spin are shown in Fig. 1, which shows spin splitting of the energy bands due to the intrinsic SOC. Protected by the time-reversal ($\mathcal{T}$) symmetry, the band energies in the K- and K'-valleys are identical but the spins are reversed as illustrated in Fig. 1.

In the presence of an external field, $\mathbf{F}(t)$, the Hamiltonian in the length gauge is $H_0(\mathbf{k}) + H^{\text{int}}$, where $H^{\text{int}} = e\mathbf{F}(t)\mathbf{r}$, and e is unit charge. Electron dynamics in the presence of field $\mathbf{F}(t)$ includes two major components: intraband and interband. The intraband electron dynamics in a single band is described by the Bloch acceleration theorem, $\mathbf{k}(\mathbf{q}, t) = \mathbf{q} + \frac{e}{\hbar c}\mathbf{A}(t)$, where $\mathbf{k}(\mathbf{q}, t)$ is electron crystal momentum as a function of time t, $\mathbf{q}$ is the initial crystal momentum, $\mathbf{A}(t) = -c\int_{-\infty}^{t}\mathbf{F}(t')dt'$ is vector potential in the velocity gauge, and c is speed of light.

We describe the resulting electron dynamics by solving time-dependent Schrödinger equation (TDSE). Since the Hamiltonian, $H_0(\mathbf{k})$, is block-diagonal, the spin-up and spin-down components are decoupled. Therefore, the TDSE for each component of the spin,

$$i\hbar\frac{d\Psi}{dt} = (H^{\text{s}}_{3\times3} + H^{\text{int}})\Psi\ , \tag{8}$$

where $\text{s} \in \{\uparrow, \downarrow\}$, can be solved independently.

We solve the set of coupled ordinary differential equations (**??**)-(**??**) numerically by using a variable time step Runge-Kutta method[7] with the following initial conditions ($\beta_{v\mathbf{q}}, \beta_{c_1\mathbf{q}}, \beta_{c_2\mathbf{q}}$)=(1,0,0) to find the bands populations N as a function of time and the lattice momentum $\mathbf{q}$.

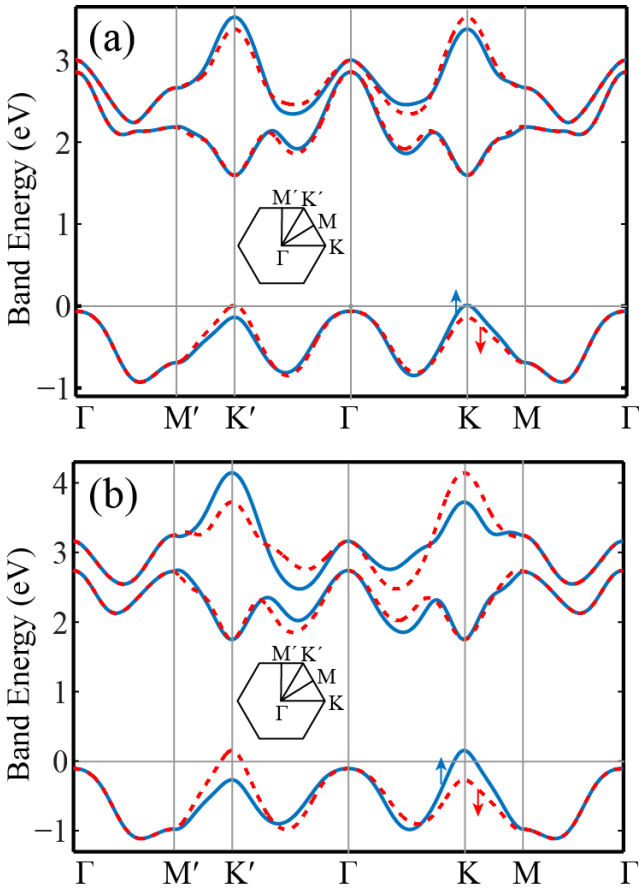

FIG. 1. (Color online) Band structure for monolayers of (a) MoS_2 and (b) WS_2 for two component of the spin. The solid lines are for spin-up and the dash lines are for spin-down.

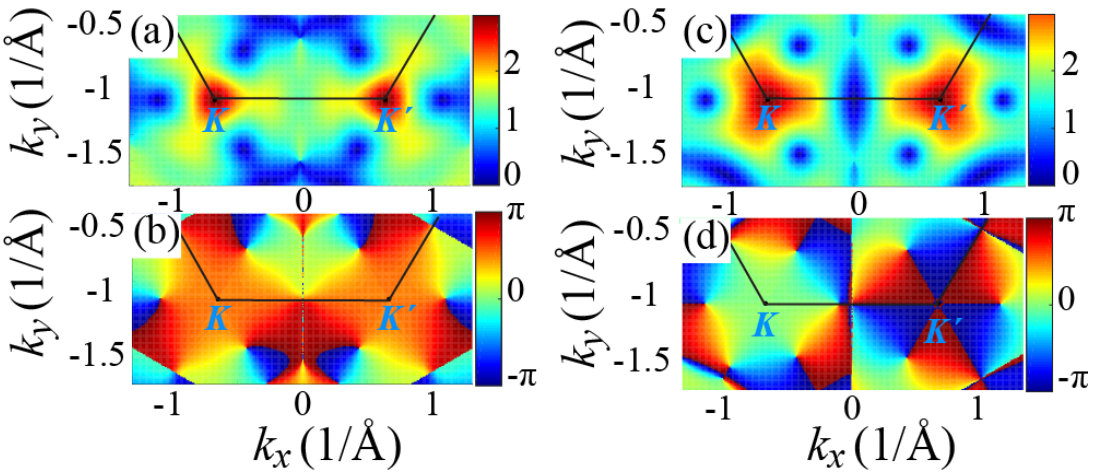

FIG. 2. (Color online) Coupling dipole matrix element $\mathbf{D}$ for MoS_2. (a) Modulus of longitudinal component, $D_k = \mathbf{D}\hat{k}$, (b) Phase of D_k, (c) Modulus of tangential component $D_\varphi = \mathbf{D}\hat{\varphi}$, and (d) Phase of tangential component D_φ calculated in the vicinity of each valley. Black solid lines show the boundary of the Brillioun zone of MoS_2.

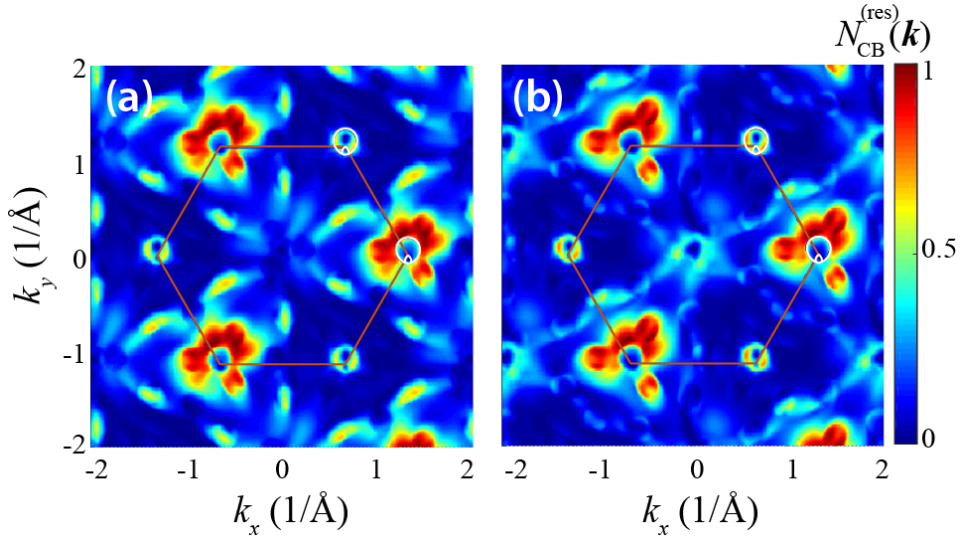

FIG. 3. (Color online) Residual CB populations $N^{(\mathrm{res})}_{\mathrm{CB,s}}(\mathbf{k})$ for monolayer MoS_2 after right-handed circularly polarized pulse with two oscillations, see Eq. (11). The red solid line shows the Brillouin zone boundary. Amplitude of the applied field is $F_0 = 0.25$ VÅ^{-1}. (a) Population $N^{(\mathrm{res})}_{\mathrm{CB}\uparrow}(\mathbf{k})$ for spin up electrons. (b) The same as panel (a) but for spin down electrons, $N^{(\mathrm{res})}_{\mathrm{CB}\downarrow}(\mathbf{k})$.

IV. MEAN FREQUECNY OF THE OPTICAL PULSE

An ultrafast pulse has no definite frequency since its Fourier component is widely distributed in the frequency space. We calculate the mean frequency, $\bar{\omega}$, of an optical pulse as

$$\bar{\omega} = \frac{\int \omega S(\omega) d\omega}{\int S(\omega) d\omega} \ , \tag{9}$$

where the pulse spectrum, $S(\omega)$, is defined as

$$S(\omega) = |\mathbf{F}_\omega|^2, \quad \mathbf{F}_\omega = \int_{-\infty}^{\infty} \mathbf{F}(t) e^{i\omega t} dt \ . \tag{10}$$

For the pulse, described in Eq. (1) of the main text, we have calculated $\hbar\bar{\omega} \simeq 1.2$ eV.

V. TWO-OSCILLATION PULSE

Here we provide a solution for a pulse which is longer than the pulse used in the main text. This pulse contains two optical field oscillations of the same chirality and is parametrized as

$$\begin{aligned} F_x(t) &= F_0 \frac{1}{12} e^{-u^2} H^{(4)}(u) \ , \\ F_y(t) &= F_0 \frac{1}{4} e^{-u^2} H^{(3)}(u) \ , \end{aligned} \tag{11}$$

where $u = t/\tau$, and $H^{(n)}$ is a Hermite polynomial of power n.

Calculated spin-resolved population distributions in the CB of MoS_2 for a two-oscillation left-handed pulse of Eq. (11) is displayed in Fig. 3. Comparing it to Figs. 2 (c), (e) of the main text, one can conclude that there is no qualitative changes in CB population distribution when extra oscillations are added to the pulse. There are some changes of the distributions along the separatrix but general picture remains the same. Namely, the K-valleys are predominantly populated outside of the separatrix. There is a very small population of the K'-valleys inside the separatrix. Overall, the valley polarization is higher that for a single-oscillation pulse. This is understandable because the two-oscillation pulse is closer to a circularly polarized CW radiation that the single oscillation one.

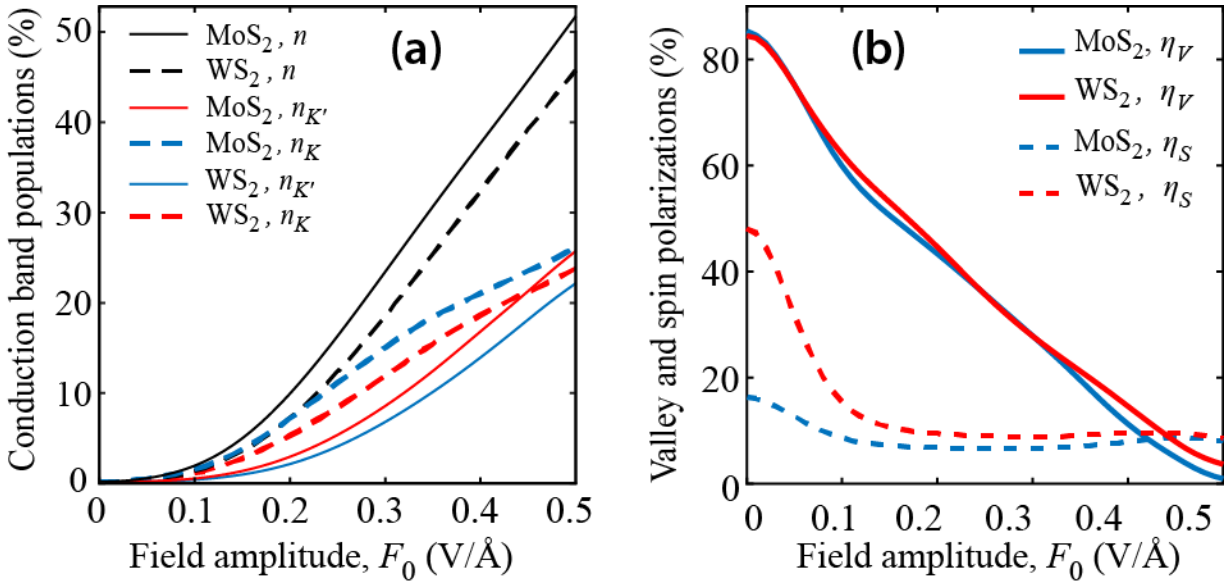

FIG. 4. Valley CB populations, valley polarization, and spin polarization for TMDC MoS_2 and WS_2, as indicated. (a) Total CB's population n and the CB's populations in the corresponding valleys as a function of amplitude F_0 of the excitation right-handed pulse, color coded as indicated. (b) Same as in (a) but for valley and spin polarizations.

VI. VALLEY AND SPIN POLARIZATION

We quantify valley polarization as

$$\eta_{\rm V} = (n^{\uparrow}_{\rm K} + n^{\downarrow}_{\rm K} - n^{\uparrow}_{\rm K'} - n^{\downarrow}_{\rm K'})/(n^{\uparrow}_{\rm K'} + n^{\downarrow}_{\rm K'} + n^{\uparrow}_{\rm K} + n^{\downarrow}_{\rm K}), \tag{12}$$

where $n^{\uparrow}_{\rm K'}$ is a CB population of the K'-valley for spin-up electrons, and similar for other populations. Likewise, we define spin polarization as

$$\eta_S = (n^{\uparrow}_{\rm K'} - n^{\downarrow}_{\rm K'} + n^{\uparrow}_{\rm K} - n^{\downarrow}_{\rm K})/(n^{\uparrow}_{\rm K'} + n^{\downarrow}_{\rm K'} + n^{\uparrow}_{\rm K} + n^{\downarrow}_{\rm K}) \ . \tag{13}$$

Figure 4 (a) displays total population $n = n_{\rm K} + n_{\rm K'}$ and valley populations $n_K = n^{\uparrow}_K + n^{\downarrow}_K$, $n_{K'} = n^{\uparrow}_{K'} + n^{\downarrow}_{K'}$ for monolayers of MoS_2 and WS_2 as functions of the amplitude, F_0, of a chiral left-handed excitation pulse. As one can see, for both TMDC's, there is a strong asymmetry in the population: the K' valley is preferentially populated. With an increase of F_0, this asymmetry decreases but the total CB population increases. A reasonable compromise is $F_0 \sim 0.25$ V/Å where the CB population is high enough ($\sim 20\%$) but valley polarization is still also high: $\eta_{\rm V} \sim 50\%$. In contrast, the spin polarization is low, $\eta_{\rm S} \sim 5\%$.

[1] G. B. Liu, W. Y. Shan, Y. G. Yao, W. Yao, and D. Xiao, "Three-band tight-binding model for monolayers of group-VIB transition metal dichalcogenides," Phys. Rev. B **88**, 085433–1–10 (2013).
[2] Roland Winkle., "Acceleration of electrons in a crystal lattice," Springer Berlin Heidelberg , 61 (2003).
[3] W. V. Houston, "Acceleration of electrons in a crystal lattice," Phys. Rev. **57**, 184–186 (1940).
[4] F. Wilczek and A. Zee, "Appearance of gauge structure in simple dynamical systems," Phys. Rev. Lett. **52**, 2111–2114 (1984).
[5] D. Xiao, M.-C. Chang, and Q. Niu, "Berry phase effects on electronic properties," Rev. Mod. Phys. **82**, 1959–2007 (2010).
[6] F. Yang and R. B. Liu, "Nonlinear optical response induced by non-Abelian Berry curvature in time-reversal-invariant insulators," Phys. Rev. B **90**, 245205 (2014).
[7] J. C. Butcher, "Coefficients for the study of Runge-Kutta integration processes," Journal of the Australian Mathematical Society **3**, 185201 (1963).